ACS APPLIED MATERIALS & INTERFACES

Research Article

www.acsami.org

Injectable Chitin-Poly(ε-caprolactone)/Nanohydroxyapatite Composite Microgels Prepared by Simple Regeneration Technique for Bone Tissue Engineering

R. Arun Kumar,[†] A. Sivashanmugam,[†] S. Deepthi,[†] Sachiko Iseki,[‡] K. P. Chennazhi,[†] Shantikumar V. Nair,[†] and R. Jayakumar*[,†]

[†]Amrita Centre for Nanosciences and Molecular Medicine, Amrita Institute of Medical Sciences and Research Centre, Amrita Vishwa Vidyapeetham University, Kochi-682041, India

[‡]Section of Molecular Craniofacial Embryology, Graduate School of Medical and Dental Sciences, Tokyo Medical and Dental University, Tokyo-113-8549, Japan

ABSTRACT: Injectable gel systems, for the purpose of bone defect reconstruction, have many advantages, such as controlled flowability, adaptability to the defect site, and increased handling properties when compared to the conventionally used autologous graft, scaffolds, hydroxyapatite blocks, etc. In this work, nanohydroxyapatite (nHAp) incorporated chitin-poly(ε-caprolactone) (PCL) based injectable composite microgels has been developed by a simple regeneration technique for bone defect repair. The prepared microgel systems were characterized using scanning electron microscope (SEM), Fourier transformed infrared spectroscopy (FTIR), and X-ray diffraction (XRD). The composite microgel, with the incorporation of nHAp, showed an increased elastic modulus and thermal stability and had shear-thinning behavior proving the injectability of the system. The protein adsorption, cytocompatibility, and migration of rabbit adipose derived mesenchymal stem cells (rASCs) were also studied. Chitin-PCL-nHAp microgel elicited an early osteogenic differentiation compared to control gel. The immunofluorescence studies confirmed the elevated expression of osteogenic-specific markers such as alkaline phosphatase, osteopontin, and osteocalcin in chitin-PCL-nHAp microgels. Thus, chitin-PCL-nHAp microgel could be a promising injectable system for regeneration of bone defects which are, even in deeper planes, irregularly shaped and complex in nature.

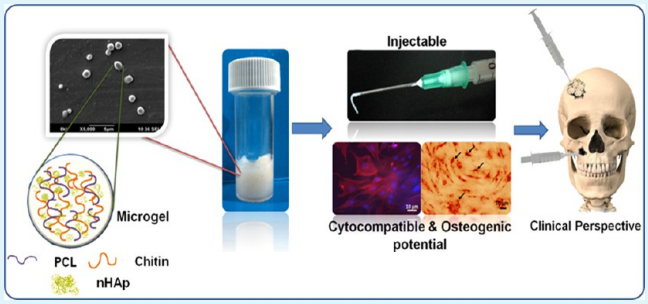

KEYWORDS: *injectable microgel, composites, hydroxyapatite nanoparticles, chitin, PCL, bone regeneration*

1. INTRODUCTION

Effective and uneventful tissue regeneration of the defects in deeper and complex bones, such as the craniofacial complex, has been a complicated issue for the clinicians.[1] This could be attributed to the skill of the surgeon who is operating; the characteristics of the tissues near the defects; and features of the defects itself, such as the size, shape, location of the defect, and type of bone involved. Above all, it depends on the choice of material which is being selected to repair/regenerate the lost bone tissue.[2] An ideal material which could be potentially used for the bone reconstruction should possess the following properties such as ease of handling, ability to fit the defect shape without any voids, lack of physical harm to the adjacent tissues, biocompatibility of the material and its degradation products, and ability to biomimic the milieu of bone.

It has been shown that the success rate is higher with the use of synthetic materials than with the use of grafts because of chances of infection, graft rejection, and defect site morbidity.[3] Therefore, graft substitutes in different forms such as blocks, powders, cements, scaffolds, and gels are being considered for the use of bone tissue engineering.[4] Currently injectable hydrogel systems from biopolymers are gaining more interest and importance for bone tissue engineering, owing to their increased biocompatibility, bioactivity, biomimicking, cost effectiveness, minimal invasiveness, and handling properties.[5,6] The gels can also be incorporated with many drug molecules, growth factors, or any bioactive molecule which could potentially aid and increase the bone regeneration.[7] Therefore, an injectable gel form was considered as it would be advantageous over other bone substitutes in terms of handling, moldability, adaptability to defect margins, increased bioadhesion, and favorable microenvironment for the cells to grow.[8]

Chitin, one of the most abundant structural aminopolysaccharides in numerous invertebrate phyla such as Cnidaria, Mollusca, Echinodermata, and Arthropoda,[9] possesses several unique properties, which favor its applications in the biomedical domain and extreme biomimetics[11] in the current scenario. Therefore, chitin was chosen to incorporate

Received: October 1, 2014
Accepted: April 20, 2015
Published: April 20, 2015

DOI: 10.1021/acsami.5b02685
ACS Appl. Mater. Interfaces 2015, 7, 9399−9409

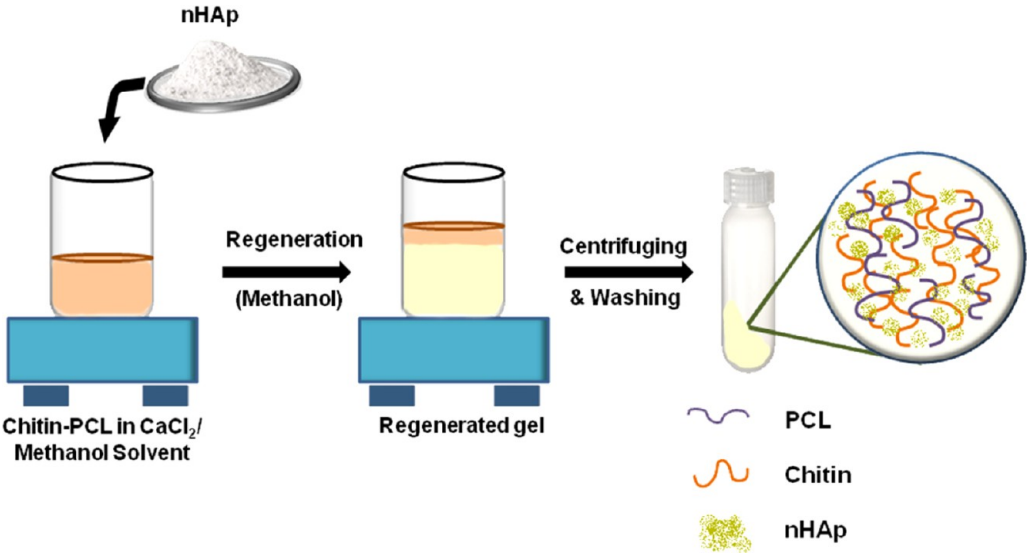

Figure 1. Schematic representation of preparation of chitin-PCL/nHAp composite microgels.

bioadhesion and biomimicking properties to the synthetic counterparts.[12] In addition, other synthetic polymers can be blended easily with chitin and can be processed into gels to improve the mechanical properties. PCL, which is FDA approved and widely being used for bone tissue engineering applications, has been blended with chitin, in order to obtain favorable viscoelastic and mechanical properties.[13] The degradation characteristics of PCL can be tuned, and its degradation products are nontoxic. PCL has a large window between its melting temperature (60 °C) and degradation temperature, and so different processing methods could be adopted. All these properties could be used advantageously to impart the necessary physical properties and degradation rates in the composite preparations.[13] Hydroxyapatite (HAp) is the natural component of bone mineral,[14] and it has been widely used for bone tissue engineering and surface modifications of implants. The inclusion of HAp has been shown to improve the cell adhesion, lead to better osteointegration, and provide a good osteoconductive environment.[15] Further, with the use of nHAp, there will be better bone healing by enhancing bioadhesion and proliferation of osteoblasts. It is also known to increase the alkaline phosphatase secretion of osteoblasts, which would help in earlier bone repair.[15] Although injectable hydroxyapatite or calcium sulfate pastes are being used to fill the bony defects, they suffer from setting shrinkage, brittleness, etc.[3,8] Therefore, a combination of polymer/bioceramics would be an ideal approach to reduce the aforementioned shortcomings and to improve osteogenesis as reported in various studies.[16,17] Considering these properties, we developed a composite microgel imparting the properties of natural polymer and synthetic polymer, reinforced with nanobiomimetic ceramic, without the use of any cross-linkers. The physicochemical properties, cytocompatibility, and osteoconductive potential of the developed chitin-PCL/nHAp microgels were analyzed. This work would provide insight into the design of injectable gels through a simple technique which would find potential application in regeneration of deeper and more complex shaped bone defects.

2. EXPERIMENTAL SECTION

2.1. Materials. α-Chitin was obtained from Koyo Chemical Ltd., Japan, with degree of acetylation >85%. PCL (molecular weight 43 000−50 000) was purchased from Polysciences Inc., Warrington, PA. Hydroxyapatite nanopowder (<200 nm) and *para*-nitrophenylphosphate (PNPP) substrate were purchased from Sigma-Aldrich. Calcium chloride dihydrate and methanol were purchased from Merck Chemicals. Alamar Blue, trypsin-EDTA, DAPI, Pen-Strep, and fetal bovine serum (FBS) were obtained from Gibco, Invitrogen Corporation. Milli-Q water (18.2 MΩ cm) was used wherever needed. All chemicals were used with no further modifications and purification.

2.2. Methods. *2.2.1. Microgels Preparation.* Chitin-PCL microgels (hereafter referred as control microgels) and chitin-PCL-nHAp composite microgels (hereafter referred as composite microgels) were synthesized by the solvent regeneration method.[18] Chitin was dissolved in saturated $CaCl_2$/methanol solvent to obtain a 0.5% (w/v) chitin solution. PCL (1% w/v) was separately dissolved in the saturated $CaCl_2$/methanol solvent under constant stirring and heating (60 °C). nHAp powder was dispersed uniformly in the chitin solution. Pure chitin solution or chitin solution dispersed with nHAp was added to the PCL solution in order to prepare the control and composite microgels, respectively. The weight ratio of chitin, PCL, and nHAp was 2:1:0 and 2:1:1, for control microgels and composite microgels, respectively. After the chitin solution was added to the dissolved PCL solution, it was kept under constant stirring for proper blending of the two polymer solutions. Then, excess of methanol (volume equivalent to the initial chitin solution taken) was added to chitin-PCL solution, until the gel was regenerated. This was centrifuged and washed with water, several times in order to remove methanol and calcium chloride. The obtained gel was resuspended in water and probe sonicated to obtain the microgels. This was again centrifuged to obtain a uniform microgel (Figure 1). This was used for further physicochemical characterization studies. For *in vitro* studies, the required amount of microgels was UV sterilized.

2.2.2. Microgel Physicochemical Characterizations. The size and shape morphologies of the prepared microgel particles were characterized by SEM (JEOL JSM-6490LA Analytical SEM). Briefly, 1 mg of the prepared microgels was uniformly suspended in 10 mL of water. This suspension was further diluted to a 1:15 ratio. From this, a few drops were drop casted, air-dried, gold sputtered, and imaged. FTIR was carried out on a Shimadzu IRAffinity-1S Fourier transform infrared spectrophotometer, in order to compare functional groups in control and composite microgels and to confirm the incorporation of the nHAp particles in the microgels. The microgels were lyophilized for 24 h and were subjected to FTIR. The infrared spectrum

DOI: 10.1021/acsami.5b02685
ACS Appl. Mater. Interfaces 2015, 7, 9399−9409

(transmittance) was recorded from 4000 to 400 cm^{-1}. Further X-ray diffraction (XRD) analysis was carried out between 2θ values of 5° to 55° using PAN analytical X'Pert PRO X-ray diffractometer, in order to confirm the characteristic diffraction peaks of chitin, PCL, and nHAp in the microgels.

2.2.3. Rheological Studies of the Microgels. 2.2.3.1. Viscoelastic Study. Further rheological studies were carried out and analyzed using a Malvern Kinexus pro rheometer. All studies were carried out using a stainless steel 20 mm cone plate (4°) (upper), and the gap between the upper and lower plates was kept at 0.5 mm. The temperature was maintained at 25 °C.

Amplitude sweep was carried out starting from a strain percentage of 10^{-1}, and the instrument was set to automatically determine the end of the linear viscoelastic region (LVER). Elastic modulus (G'), viscous modulus (G''), and phase angle (δ) were measured against varying percentages of shear strain. Frequency sweep was carried from 10^{1} to 10^{-1} Hz in the LVER region of the microgels to determine the gel strength and other rheological characteristics of the microgel.

2.2.3.2. Temperature Stability Tests. The microgels were subjected to different ranges of temperature from 25 to 38 °C under constant frequency and shear; complex modulus and complex viscosity were measured. This was done to test the stability of the microgels from room temperature to normal body temperature.

2.2.3.3. Flow Curve Analysis and Injectability. The viscosities of the control and composite microgels were plotted against varying shear rates of 10^{-1} to 10^{-2} s^{-1} to obtain the flow curves. The temperature was maintained at 25 °C. Further, to test the injectability, the microgels were loaded into 1 mL syringes (flowing under shear), without a needle (less shear) and through a needle (21G) (high shear), and the flow was observed visually. This helps to determine the flow behavior and injectability of the prepared microgels.

2.2.3.4. Inversion Study. Inversion study was carried out in order to test the microgel's flow under the influence of gravity. This analysis simulates the microgels being placed in the defect after injecting. This was carried out by placing equal quantities of control and composite microgels in cylindrical bottles with flat base. After the microgels have been leveled, the bottles were inverted to stand on their caps, and they were left undisturbed.[19] The flow of microgels was observed at different time points (0, 2, 48, and 100 h).

2.2.4. Protein Adsorption Studies. Equal quantities of control and composite microgels were placed in a 96 well plate, and this was allowed to dry in a hot air oven. To each sample complete Dulbecco's modified Eagle's medium (DMEM) was added, and incubated at 37 °C for different incubation time points (0.5, 2, and 6 h). After the incubation periods, the medium was removed, and BCA reagent was added and incubated for 30 min at 37 °C. Aliquots were taken, and the adsorbed protein was quantified using a bicinchoninic acid (BCA) assay. The principle of this assay is based on the reduction of Cu^{2+} to Cu^{1+}, and the absorbance was read at a wavelength of 562 nm after the incubation.[20]

2.2.5. Cell Viability Evaluation. Alamar blue assay was used to measure cell viability. Alamar blue reagent is a cell viability and cell proliferation indicator that uses the inherent reducing power of live cells as an indicator of metabolic activity. Rabbit adipose derived mesenchymal stem cells (rASCs) were used to carry out the cell viability study. rASCs were isolated from adipose tissue collected from euthanized New Zealand albino rabbits after the ethical consent was obtained from the institutional body of Amrita Institute of Medical Sciences. Cell isolation was done with a previously reported technique with modifications,[21] by treating the tissue with 0.25% collagenase following which the cells were pelleted, redispersed, and seeded. rASCs were cultured in 25 cm^2 flasks, and the cells were trypsinized after reaching a confluency of 80%. rASCs were maintained in DMEM containing 10% FBS and 100 U/mL penicillin−streptomycin. Measured quantities of sterilized control and composite microgels were dispersed in the complete DMEM. The cells were seeded in 24 well plate with a density of 5×10^4 cells per well. After the cells adhered, the medium was removed, and it was replaced with the microgel dispersed media. This was then incubated at 37 °C for the required time periods (24 and 48 h). After the required time periods, the culture medium was replaced with a serum free medium containing 10% alamar blue reagent, and this was incubated at 37 °C for 5 h. After the incubation, the viability of the cells was measured by reading the optical density at 570 nm with 600 nm taken as the reference wavelength using a microplate spectrophotometer (Biotek Power Wave XS).[22]

2.2.6. Cell Migration Evaluation. Cell migration was checked by conducting a scratch assay. rASCs were seeded in a 24 well plate with seeding density of 5×10^4 cells per well. The cells were incubated in DMEM and were allowed to become confluent. After confluency, the DMEM was removed, and a uniform scratch was made using a 100 μL pipet tip. The microgels were dispersed in DMEM, added to the wells, and incubated at 37 °C. The proliferation and migration of the cells into the scratched space were assessed after 24 and 48 h.[23]

2.2.7. Cell Attachment. Cell attachment studies were carried out to assess the cell adhesion on the gel. Glass coverslips were coated with the control and composite microgels and were partially dried at room temperature. Then, 5×10^4 cells were seeded over the microgels' surfaces. After 1, 6, and 24 h, the cells were stained for actin filaments and nucleus using TRITC conjugated phalloidin stain and DAPI, respectively, and were observed under fluorescence microscope.

2.2.8. Cell Differentiation. The cell differentiation study was carried out to evaluate the effect of the microgels during the differentiation process of the rASCs into osteoblasts. The cells were seeded in a 24 well plate at a density of 5×10^4 cells/well and allowed to become confluent. After the cells were confluent, the medium was replaced with osteogenic media, and osteogenic media dispersed with the control and composite microgels. Media were replenished once every 2−3 days. Alkaline phosphatase (ALP) is one of the important biomarkers which can give the level of osteodifferentiation and endogenous mineralization. Therefore, ALP levels were analyzed after 7, 14, 21, and 28 days. The cells were lysed by 1% triton x-100. In a 96 well plate, 50 μL of the liquid substrate (PNPP) was added followed by 80 μL of glycine buffer. A 50 μL of the lysate was added to this and incubated in the dark for 30 min. The absorbance was measured at 405 after adding 20 μL of stop solution (5 M NaOH). The mineralization associated with the osteoblastic activity was assessed by alizarin red S staining. Alizarin red S forms a complex with calcium in a chelation process. On the 14th day the cells cultured in coverslips were washed with PBS and fixed with 4% PFA. It was then washed with ice cold distilled water and stained with 2% alizarin red S (pH 4.2). The coverslips were rinsed with distilled water and observed under a microscope.[24]

2.2.9. Immunocytochemical Staining. The expression of bone specific proteins such as ALP, osteocalcin (OCN), and osteopontin (OPN) were analyzed by immunoflouresence. The rASCs were cultured in osteogenic media with the same protocol which was followed for cell differentiation studies. The expression of ALP was analyzed by tagging with anti-ALP antibody (Sigma-Aldrich) at the end of 7 days. The osteocalcin and osteopontin expressions were analyzed by tagging with anti-osteocalcin (Pierce Antibodies) and anti-osteopontin (OriGene Technologies, Inc.) at the end of 21 days. Briefly, the PFA fixed sampes after permeabilization with 0.5% Triton x-100 and blocking with 3% bovine serum albumin (BSA) were incubated with the primary antibodies as per manufacturers' recommended dilution overnight. Secondary antibodies used were donkey antigoat IgG (Santa Cruz) and goat antimouse IgG (Abcam) conjugated with FITC following 1:200 and 1:1000 dilutions, respectively. All the samples were counterstained for actin filaments using TRITC conjugated phalloidin (Invitrogen) and were analyzed under fluorescence microscope.

2.2.10. Statistical Analysis. All computable results were achieved after triplicate samples. Data were articulated by the mean ± standard deviation. Paired Student's two-tailed t test was carried out in order to assess the statistical significance, wherever necessary and applicable. A value of $p < 0.05$(*), $p < 0.01$(**), and $p < 0.001$(***) was measured to be statistically significant.

DOI: 10.1021/acsami.5b02685
ACS Appl. Mater. Interfaces 2015, 7, 9399−9409

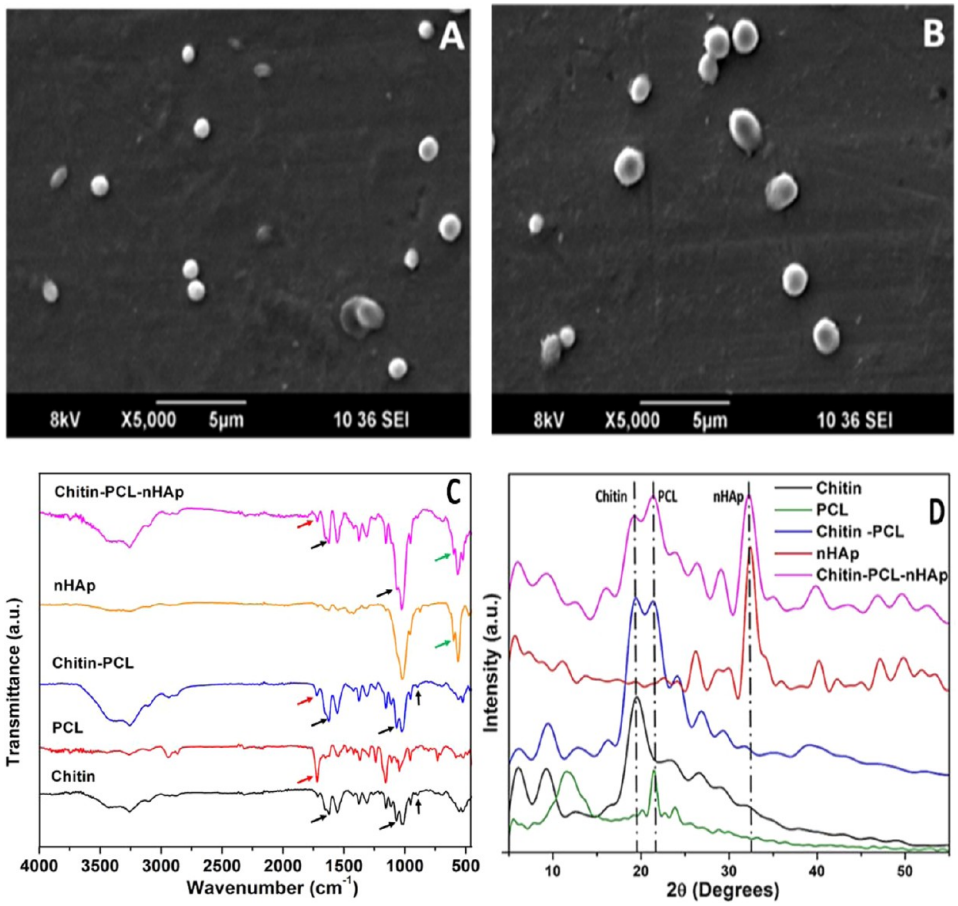

Figure 2. Scanning electron micrographs of chitin-PCL microgel particles (A) and chitin-PCL-nHAp microgel particles (B). FTIR spectra (C). Black, red, and green arrows indicative of chitin, PCL, and nHAp peaks, respectively. XRD analysis (D).

3. RESULTS AND DISCUSSION

3.1. Preparation of Chitin-PCL and Chitin-PCL/nHAp Microgel. Control and composite microgels were prepared by simple regeneration chemistry. The dissolved chitin and PCL solutions blend together, and physical interlocking of the polymer chains occurs. When excess of methanol was added, the chitin-PCL blend regenerates in the gel form. The interaction between chitin and PCL probably occurs through hydrogen bonding among carbonyl groups of PCL with hydroxyl and amide groups present in chitin.[25] The nHAp will possibly get entrapped between the polymer matrices; thereby, nHAp is being incorporated into the polymer. Further, the gel was subjected to probe sonication at an optimized amplitude and time, which resulted in the polymer matrices being in the required micron size, thereby resulting in microgels.

3.2. Physicochemical Characterizations of Microgels. The particle size and morphology, which were analyzed by SEM, showed that the particles were almost spherical in shape, and the diameters of the control and composite microgels were found to be 1 ± 0.2 μm and 1.5 ± 0.2 μm, respectively (calculated using ImageJ software) (Figure 2A,B). The slight increase in size of the composite microgels could possibly be because the nHAp particles would have been trapped between the polymer matrices of the microgel thereby leading to an increase in the space between the polymer chains and slightly increasing the size.

The analysis of the FTIR data is shown in Figure 2C. The control microgel showed the characteristic peaks of chitin and PCL. The peaks at 3450, 3102, 2945, 2872, 1660, 1465, 1112, and 895 cm^{-1} were all characteristic peaks of chitin. The observed peaks at 1730 and 1035 cm^{-1} indicate the presence of PCL. The increase in peak intensity was observed at the 3500−3200 cm^{-1} region, indicating the intermolecular hydrogen bonding between chitin and PCL.[25,26] In addition, the nHAp incorporated composite microgel showed the characteristic double peak at 603 and 567 cm^{-1} which corresponds to the bending vibrations of P−O bond. The peak at 1035 cm^{-1} also corresponds to the stretching vibration of the P−O bond.[27] These results confirm that nHAp particles have been incorporated into the chitin-PCL microgels' matrix.

The XRD analysis showed that the diffraction peaks at 19°, 22°, and 32° are present in the composite microgels which correspond to the characteristic peaks of chitin, PCL,[28] and nHAp, respectively.[29] This confirms that nHAp has been incorporated into the chitin-PCL matrix (Figure 2D).

3.3. Microgels Rheological Studies. *3.3.1. Viscoelastic Study.* The viscoelastic analysis was carried out by applying varying amplitudes of shear strain (%) to find the LVER. These are shear strain percentages at which the sample can elastically strain and can return back to its original state once the stress is removed. The further oscillation studies should ideally be done within the LVER.

The experiment revealed that the LVERs of control and composite microgels were in the same shear strain range

DOI: 10.1021/acsami.5b02685
ACS Appl. Mater. Interfaces 2015, 7, 9399−9409

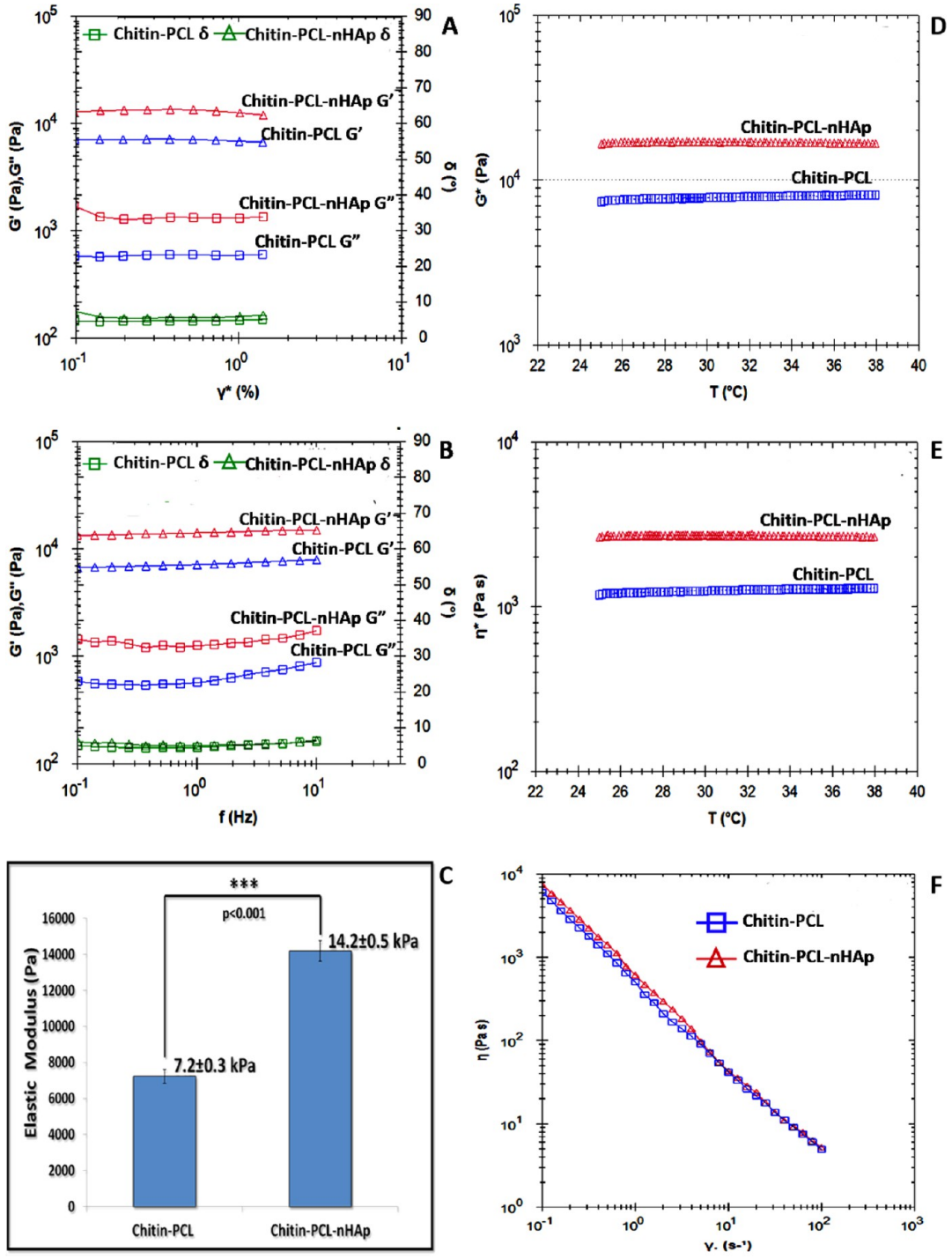

Figure 3. Rheological characterizations of microgels: amplitude sweep (A), frequency sweep (B), comparison of elastic modulus (C), complex modulus (G^*) vs temperature (D), complex viscosity (η^*) vs temperature (E), and flow curves (F).

(Figure 3A). This indicates that the addition of nHAp does not alter the viscoelastic behavior of the microgels. Further, the frequency sweep was carried out using the shear stress values only in the LVE range. Frequency sweep helps to determine the gel strengths (elastic and viscous modulus) and phase angle which will determine the physical nature of the microgels. It was found that for both the microgels G' was greater than G'', which indicates that the microgels were dominated by the elastic component, which is the characteristic feature of gels (Figure 3B). The phase angle (δ), which was around 5°, indicated that the microgels were solid dominating with a fluid component. (If δ = 0°, then it is solid, and if δ = 90°, it is liquid.[30]) This means that the microgels will not flow unless a shear stress is otherwise applied. It was also found that the elastic modulus (G') values of control and composite microgels were 7.2 ± 0.3 and 14.2 ± 0.5 kPa, respectively, which was statistically significant with p value <0.001 (Figure 3C). The increase in the elastic modulus should be due to the addition of nHAp particles, which act as reinforcements to the polymeric matrix without changing the viscoelastic nature of the matrix.

3.3.2. Temperature Stability Tests. The temperature ramp studies indicate that the complex modulus (G^*) of the control

DOI: 10.1021/acsami.5b02685
ACS Appl. Mater. Interfaces 2015, 7, 9399−9409

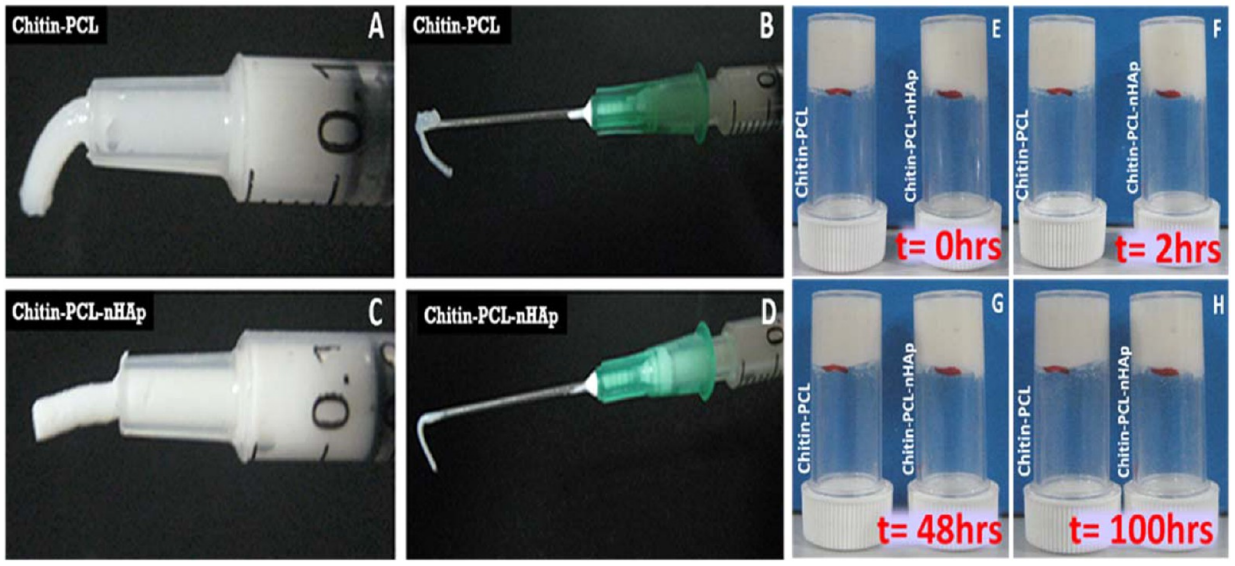

Figure 4. Injectability of the chitin-PCL microgels and chitin-PCL-nHAp microgels through a syringe without needle (A, C) and with needle (B, D). Inversion test showing the stability of microgels against gravity at different time points (E–H).

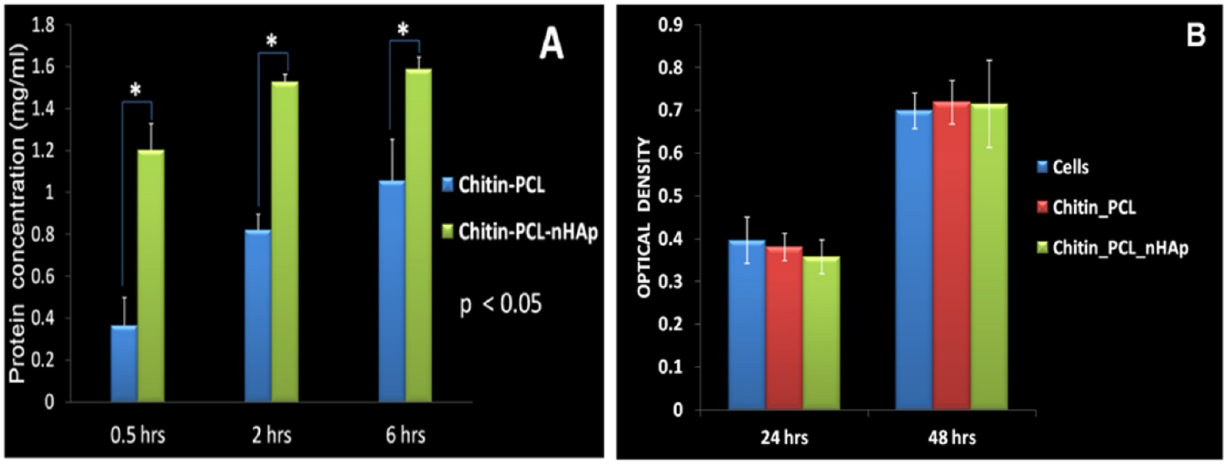

Figure 5. Serum protein adsorption on control and composite microgels for different time points analyzed by BCA assay (A) and rASCs viability determined by Alamar Blue assay in the presence of control and composite microgels for predetermined time points (B).

and composite microgels was stable throughout the range 25–38 °C. This shows that the microgels did not show any changes in the gel strengths at room temperature and normal body temperature. The same pattern was also observed for the complex viscosity (η^*) which indicated that the viscosity also did not change with temperature (Figure 3D,E). This is a very much desired property because the composite microgels could be stored in room temperature conditions and will still retain the viscoelastic properties as prepared, even after being placed into the body.

3.3.3. Flow Curve Analysis and Injectability. The change in viscosity (Pa s) with respect to the shear rate (s^{-1}) gives the flow curves of the control and composite microgels. Flow curves of both the microgels indicated that the viscosity reduces as the shear rate is being increased from 0.01 to 100 s^{-1}. This indicated that the microgels were non-Newtonian fluids and exhibited a shear-thinning property; i.e., as the shear is being increased the gel will flow (Figure 3F).[31] This is the most required property for an injectable material. As the shear is applied to the microgels by the syringe plunger, it will smoothly flow out of the syringe. The higher the shear rate, the lower the viscosity will be; thus, flow will be higher. The control and composite microgels, showed a smooth injectability without any break in the flow, through the nozzle of the syringe (Figure 4A,C). The smooth and continuous injectability was also observed when tested through a 21G needle (Figure 4B,D). This was seen to be consistent with the data observed from the flow curves of the microgels. Further, the microgels retained their shape and did not flow on their own after being ejected from the syringes. This shows that the microgels could be easily injected into inaccessible locations, and they could adapt to the defect shape by applying required shear. Further, after being placed into the defect, the nHAp composite microgels have enough adhesive nature to the bone defect margins and thus will stay without flowing into the adjacent tissue, at normal body temperature.

3.3.4. Inversion Study. The inversion study revealed that both the microgels did not flow under the influence of gravity even after 100 h (Figure 4E–H). This indicates that the microgels once placed in a defect area will not flow to the adjacent areas. This indicated that the yield stress of the microgels was greater than that of the gravitational stress,[19] and

DOI: 10.1021/acsami.5b02685
ACS Appl. Mater. Interfaces 2015, 7, 9399–9409

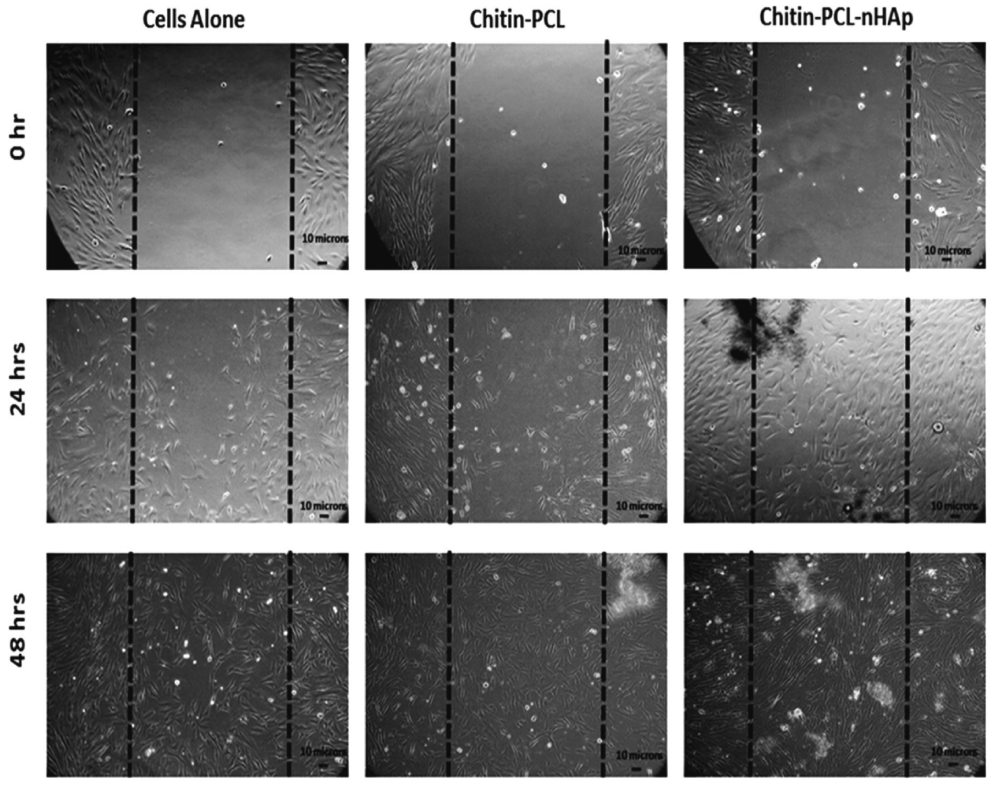

Figure 6. Scratch assay for assessing the migration of rASCs for different time points.

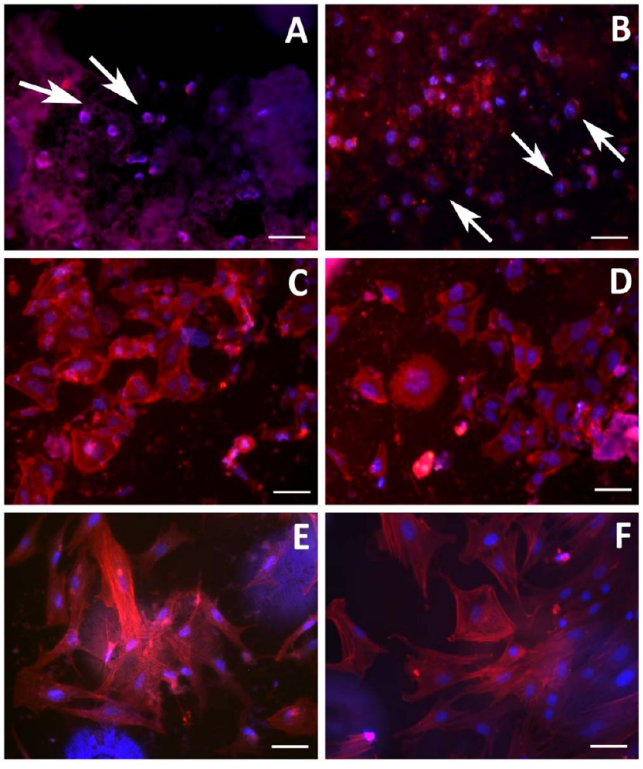

Figure 7. Actin (red) and nucleus (blue) stained cells visualized under fluorescent microscope for cell attachment after 1 (A, B), 6 (C, D), and 24 (E, F) hours. Cells seeded over chitin-PCL coated coverslip (A, C, E) and cells seeded over chitin-PCL-nHAp coated coverslip (B, D, F). Scale bar indicates 50 μm.

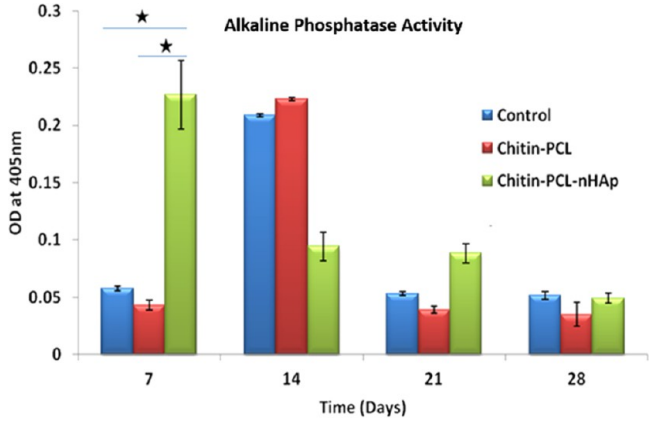

Figure 8. ALP activity for cells treated with control and composite microgels compared with cells alone in osteogenic media over different time points. Cells treated with composite microgels show significant increase in ALP activity at day 7 compared to controls (significance compared over control samples with 95% confidence).

therefore, there is no disruption of the polymer matrix itself. Also, the adhesion of the microgels to the walls of the container was high enough to hold the microgels in its place without flowing. This substantially depends on the ratio of the water to the polymer matrix present in the microgels. This is one of the expected properties for an injectable gel material, because this will make the microgels flow only when shear is applied and helps to retain its shape after being injected into the site. This makes sure that the gel will be in the place where it is intended to be and will not flow into the adjacent tissues, unless shear is applied.

3.4. Protein Adsorption. Protein adsorption was carried out for the control and composite microgels and was quantified

DOI: 10.1021/acsami.5b02685
ACS Appl. Mater. Interfaces 2015, 7, 9399−9409

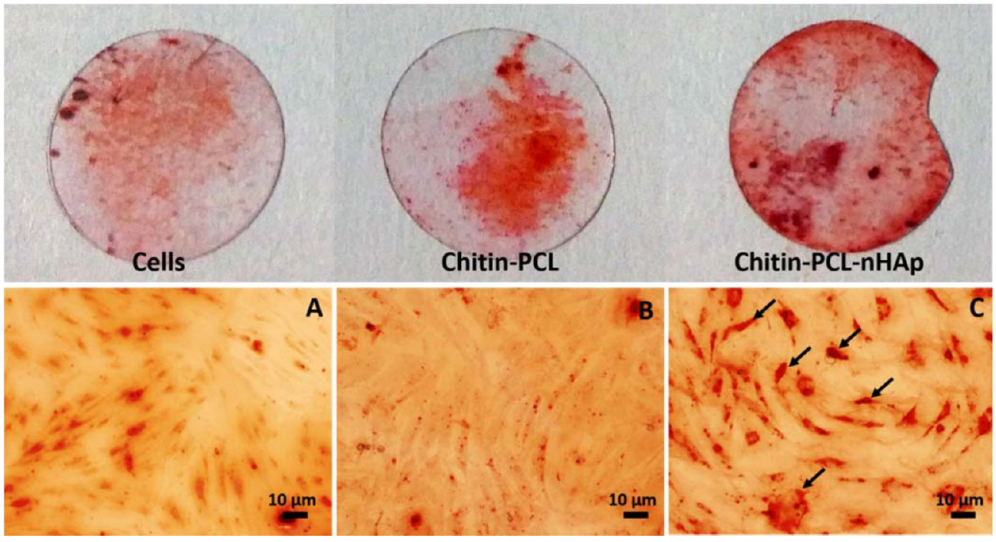

Figure 9. Alizarin Red S staining after 14 days. First row shows the photographic appearance of alizarin red S stained coverslips containing cells treated with osteogenic medium containing control and composite microgels. Second row shows the bright field image of alizarin red S stained cells exposed to osteogenic medium alone (A), chitin-PCL control microgels (B), and chitin-PCL-nHAp composite microgels (C) which show dark red spots (black arrow) indicating higher mineralization and cell morphology similar to osteoblasts.

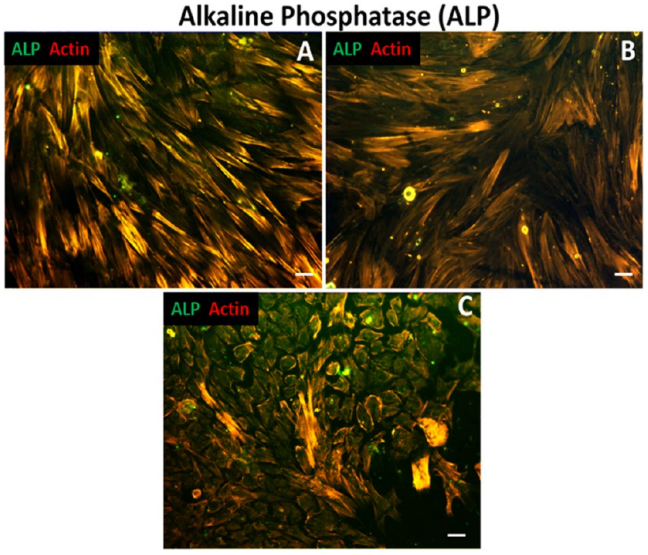

Figure 10. Immunocytochemical staining indicating the ALP expression after 7 days in cells alone (A), cells exposed to control gel (B), and cells exposed to composite gel (C). Scale bar indicates 50 μm.

after 0.5, 2, and 6 h using a BCA assay. It was observed that there was significantly ($p < 0.05$) larger quantity of protein being adsorbed in the composite microgels (Figure 5A) due to the incorporation of nHAp. The nHAp has a higher surface to volume ratio, thereby resulting in more sites for protein binding.[32] The presence of nHAp enhanced the protein binding through the electrostatic interactions between the phosphate group and the amino group of the proteins.[33] The protein content adsorbed at 2 and 6 h was almost the same, and this would probably be because of the saturation of the adsorption sites after 2 h. Thus, the composite microgels, which showed more protein adsorption, would be favorable for tissue engineering applications because the higher amount of protein adsorbed and the lesser time taken for the protein adsorption indicates that more cell adhesion can take place and therefore better bioactivity could be expected.

3.5. Cytocompaibility Evaluation. The cell viability was carried out using Alamar Blue assay for 24 and 48 h. The results indicate that both control and composite microgels show no significant changes in the cell viability as compared with that of the positive control (cells + media) (Figure 5B). This indicated that both control and composite microgels were cytocompatible in nature.

3.6. Cell Migration. The cell migration studies of the prepared microgels were carried out using scratch assay. The scratched area was visually analyzed under optical microscope post 24 and 48 h. It was observed that composite microgels showed more proliferation and migration when compared with control microgel and cells alone after 24 h (Figure 6). The increased migration of cells in composite microgels at 24 h could probably be explained by the increased protein adsorption on nHAp, as observed in the protein adsorption studies. It has been previously reported that HAp could adsorb adhesion proteins such as fibronectin, vitronectin on its surface. This would favor better cell adhesion and migration.[34,35] Initial faster migration and proliferation in the presence of nHAp would be an ideal requisite when considering the *in vivo* environment because the MSCs around the defect could migrate and proliferate faster, thereby aiding in efficient reconstruction. However, after 48 h, the cells incubated with the control and composite microgels showed complete closure of the scratch. The complete closure of the scratch in the cells treated with both control and composite microgels after 48 h indicates that the presence of *N*-acetyl-glucosamine and *N*-glucosamine in chitin enhances the cell migration and proliferation as it mimics the ECM.[36]

3.7. Cell Attachment. For analysis of the cell responsiveness toward the material, fluorescent microscopic images of cell attachment at various time intervals were taken. In the first hour, more cell spreading was seen in the sample containing nHAp (Figure 7B, arrows) compared to control gel (Figure 7A, arrows). In 6 h almost similar cell spreading was observed (Figure 7C,D). Complete and well-spread morphology was

DOI: 10.1021/acsami.5b02685
ACS Appl. Mater. Interfaces 2015, 7, 9399−9409

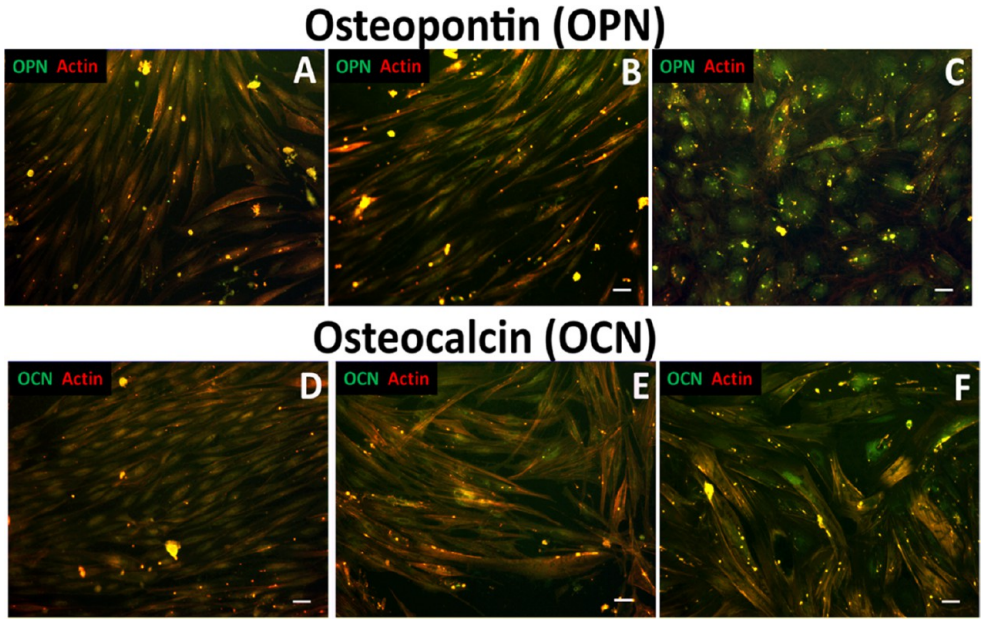

Figure 11. Immunocytochemical staining indicating the osteopontin (A−C) and osteocalcin (D-F) expression after 21 days in cells alone (A, D), cells exposed to control gel (B, E), and cells exposed to composite gel (C, F). Scale bar indicates 50 μm.

seen in both control and composite microgels after 24 h (Figure 7E,F). The nuclei of the cells were also observed to have normal morphology (Figure 7C−F). In composite microgels a well-defined actin filament assembly was observed in the same (Figure 7B,D,F). This indicates that the composite microgels have a very good cell adhesion interface compared to that of the control. This property could be mainly attributed to the well-known fact that chitin and nHAp enhance the cell adhesion.[37] This implies that when the composite microgels are placed in the tissue defect, it would help the migrated cells to attach and adhere onto the microgels and promote bone regeneration.

3.8. Cell Differentiation. The analysis of ALP levels revealed that the cells alone and cells exposed to control microgels showed a typical rise of ALP level during the 14th day[38] and thereafter a decrease in the ALP level (Figure 8). This indicates that control microgels do not affect the osteodifferentiation process and mineralization takes place after the 14th day. Interestingly, the cells exposed to composite microgels showed an increase in the ALP level during the seventh day followed by a reduction. This indicates that the cells tend to show an accelerated differentiation and an early onset of maturation phase. To confirm this phenomenon Alizarin Red staining (Figure 9) was done on cells at the 14th day time point. A dense staining of calcium deposits was observed in cells in the presence of composite microgels, when compared to the cells alone and control microgels. This confirms that the cells in contact with the composite microgels have reached the maturation phase, where it has started to deposit calcium containing minerals. Microscopic examination of the same revealed the cells had osteoblast-like morphology and more foci of mineral deposition were present in the composite microgel exposed cells. Thus, the cells in contact with the composite microgels showed earlier, denser, and increased foci of mineralization which is comparable with the other studies.[39] This would be due to the presence of nHAp, which increases the surface area and also increases the number of nucleation points for the mineral deposition by the cells. Furthermore, presence of nHAp serves as the source for calcium and phosphate ions, which would facilitate the cells for early differentiation and increased mineralization, when compared to microgels without nHAp and cells alone.[40,41] Thus, the presence of composite microgels would enhance the differentiation rate and mineral deposition by the osteoblasts, thereby aiding in faster and enhanced bone regeneration.

3.9. Evaluation of Immunocytochemical Staining. The differentiation of rASCs to osteoblasts was further confirmed by immunostaining of specific proteins that gets expressed at different time points. Early marker expression was evaluated by ALP expression in 7 days as per the pattern observed in the above study. Differentiation in the presence of composite microgel showed an accelerated pattern. Significant expression of ALP was observed in the cells cultured in the presence of composite microgel (Figure 10C) when compared to those from cells alone (Figure 10A) and in the presence of control gel (Figure 10B).

The expression of late markers indicating the differentiation into osteoblasts was analyzed after 21 days and is represented in Figure 11. Osteopontin (OPN) expression was observed significantly in the cytoplasm of cells cultured in the presence of composite microgel. The presence of nHAp played a significant role in enhancing osteogenesis, thus showing significant increase in expression of osteopontin (Figure 11C). Similar expression pattern was observed for osteocalcin (Figure 11D−F). Inorganic phosphate, which is an integral component of nHAp, is suggested to have a specific role in osteoblast function in differentiation and bone remodeling *in vivo*.[42] The relationship of expression of osteogenic factors during cell growth and differentiation has been studied elaborately.[42] The osteogenic differentiation phase is divided into three, viz., cell proliferative phase, extracellular matrix maturation phase, and mineralization phase. Our results demonstrate that the presence of nHAp in the culture conditions induced an early hike of ALP levels followed by its decline. This is indicative of the end of cell proliferative and extracellular matrix maturation phase. The enhanced expression

DOI: 10.1021/acsami.5b02685
ACS Appl. Mater. Interfaces 2015, 7, 9399−9409

of osteopontin and osteocalcin in cells cultured in the presence of composite microgels indicates significant cell maturation and mineral deposition during the mineralization phase. Moreover, the reciprocal relationship between the ALP activity and mineralization observed in our study confirms the typical osteogenic differentiation pattern.[42−44] As a summary of these results, the presence of nHAp induced an early osteogenic differentiation of rASCs, which implies that the composite microgel would favor early bone regeneration.

4. CONCLUSIONS

Injectable chitin-PCL-nHAp microgels system was synthesized without any cross-linkers using regeneration chemistry. The chitin-PCL and chitin-PCL/nHAp composite microgels were characterized using SEM, FTIR, and XRD and confirmed the incorporation of nHAp into chitin-PCL matrix. Rheological studies showed that nHAp containing microgels showed an increased elastic modulus without a change in the other properties. The properties of control and composite microgel (G^* and η^*) were stable from 25 to 38 °C. The microgels exhibit a shear-thinning behavior, and flow was observed only under shear stress, which indicates the composite microgels could potentially be a good choice for injectable material for non-load-bearing applications. The protein adsorption was found to be higher for composite microgels when compared to that for chitin-PCL microgels, which proves that addition of nHAp will improve the cell adhesion and thereby better bioactivity. The prepared composite microgel was cytocompatible and showed enhanced cell migration and proliferation, and increased mineralization was observed, which is a required characteristic for bone tissue regeneration. Additionally, immunofluorescence imaging studies of ALP, OCN, and OPN confirmed the enhanced osteogenic potential of composite microgel. These results indicated that the synthesized injectable chitin-PCL-nHAp composite microgels could be potentially used for the regeneration of bone defects. Further, this system is also a promising platform to carry out further work such as incorporation of growth factors or drugs such as antibiotics, etc., in order to improve the healing and regeneration potentials.

AUTHOR INFORMATION

Corresponding Author

*E-mail: rjayakumar@aims.amrita.edu, jayakumar77@yahoo.com. Phone: +91-484-2801234. Fax:+91-484-2802020.

Author Contributions

R.A.K., A.S., and S.D. contributed equally.

Notes

The authors declare no competing financial interest.

ACKNOWLEDGMENTS

The authors are thankful for the support provided by Nanomission, Department of Science and Technology (DST), Government of India, under the "Thematic Unit of Excellence" program. R.J. and S.I. are thankful for the support provided by the Department of Science and Technology (DST, India) and Japan Society for the Promotion of Science (JSPS) joint research program (File No. DST/INT/JSPS/P-160/2013). S.D. is grateful to the Council of Scientific and Industrial Research for financial support under the CSIR-SRF Award 9/963(0034)2K13-EMR-I. The authors are also thankful to Mr. Sajin P. Ravi for his help in SEM imaging.

REFERENCES

(1) Artico, M.; Ferrante, L.; Pastore, F. S.; Ramundo, E. O.; Cantarelli, D.; Scopelliti, D.; Iannetti, G. Bone Autografting of the Calvaria and Craniofacial Skeleton. *Surg. Neurol.* **2003**, *60*, 71−79.

(2) Stevenson, S.; Emery, S. E.; Goldberg, V. M. Factors Affecting Bone Graft Incorporation. *Clin. Orthop. Relat. Res.* **1996**, *324*, 66−74.

(3) Shah, A. M.; Jung, H.; Skirboll, S. Materials Used in Cranioplasty: A History and Analysis. *Neurosurg. Focus.* **2014**, *36*, E19.

(4) Aydin, S.; Kucukyuruk, B.; Abuzayed, B.; Aydin, S.; Sanus, G. Z. Cranioplasty: Review of Materials and Techniques. *J. Neurosci. Rural Pract.* **2011**, *2*, 162−167.

(5) Van Vlierberghe, S.; Dubruel, P.; Schacht, E. Biopolymer-Based Hydrogels as Scaffolds for Tissue Engineering Applications: A Review. *Biomacromolecules* **2011**, *12*, 1387−1408.

(6) Ni, P. Y.; Ding, Q. X.; Fan, M.; Liao, J. F.; Qian, Z. Y.; Luo, J. C.; Li, X. Q.; Luo, F.; Yang, Z. M.; Wei, Y. Q. Injectable Thermosensitive PEG-PCL-PEG Hydrogel/Acellular Bone Matrix Composite for Bone Regeneration in Cranial Defects. *Biomaterials* **2014**, *35*, 236−248.

(7) Hoare, T. R.; Kohane, D. S. Hydrogels in Drug Delivery: Progress and Challenges. *Polymer* **2008**, *49*, 1993−2007.

(8) Kretlow, J. D.; Young, S.; Klouda, L.; Wong, M.; Mikos, A. G. Injectable Biomaterials for Regenerating Complex Craniofacial Tissues. *Adv. Mater.* **2009**, *21*, 3368−3393.

(9) Ehrlich, H. Chitin and Collagen as Universal and Alternative Templates in Biomineralization. *Int. Geol. Rev.* **2010**, *52*, 661−699.

(10) Ehrlich, H.; Steck, E.; Ilan, M.; Maldonado, M.; Muricy, G.; Bavestrello, G.; Richter, W. Three-Dimensional Chitin-Based Scaffolds from Verongida Sponges (Demospongiae: Porifera). Part II: Biomimetic Potential and Applications. *Int. J. Biol. Macromol.* **2010**, *47*, 141−145.

(11) Wysokowski, M.; Petrenko, I.; Stelling, A. L.; Stawski, D.; Jesionowski, T.; Ehrlich, H. Poriferan Chitin as a Versatile Template for Extreme Biomimetics. *Polymers* **2015**, *7*, 235−265.

(12) Jayakumar, R.; Menon, D.; Manzoor, K.; Nair, S. V.; Tamura, H. Biomedical Applications of Chitin and Chitosan Based Nanomaterials—A Short Review. *Carbohydr. Polym.* **2010**, *82*, 227−232.

(13) Woodruff, M. A.; Hutmacher, D. W. The Return of a Forgotten Polymer-Poly(Caprolactone) in the 21st Century. *Prog. Polym. Sci.* **2010**, *35*, 1217−1256.

(14) Rey, C.; Combes, C.; Drouet, C.; Glimcher, M. J. Bone Mineral: Update on Chemical Composition and Structure. *Osteoporosis Int.* **2009**, *20*, 1013−1021.

(15) Zakaria, S. M.; Sharif Zein, S. H.; Othman, M. R.; Yang, F.; Jansen, J. A. Nanophase Hydroxyapatite as a Biomaterial in Advanced Hard Tissue Engineering: A Review. *Tissue Eng., Part B* **2013**, *19*, 431−441.

(16) Fu, S. Z.; Ni, P. Y.; Wang, B. Y.; Chu, B. Y.; Peng, J. R.; Zheng, L.; Zhao, X.; Luo, F.; Wei, Y. Q.; Qian, Z. Y. *In Vivo* Biocompatibility and Osteogenesis of Electrospun Poly (ε-caprolactone)-Poly-(ethyleneglycol)-Poly(ε-caprolactone)/Nano-Hydroxyapatite Composite Scaffold. *Biomaterials* **2012**, *33*, 8363−8371.

(17) Fu, S. Z.; Ni, P. Y.; Wang, B. Y.; Chu, B. Y.; Zheng, L.; Luo, F.; Luo, J. C.; Qian, Z. Y. Injectable and Thermo-Sensitive PEG-PCL-PEG Copolymer/Collagen/n-HA Hydrogel Composite for Guided Bone Regeneration. *Biomaterials* **2012**, *33*, 4801−4809.

(18) Rejinold, N. S.; Nair, A.; Sabitha, M.; Chennazhi, K. P.; Tamura, H.; Nair, S. V.; Jayakumar, R. Synthesis, Characterization and *In Vitro* Cytocompatibility Studies of Chitin Nanogels for Biomedical Applications. *Carbohydr. Polym.* **2012**, *87*, 943−949.

(19) Raghavan, S. R.; Cipriano, B. H. Gel Formation: Phase Diagrams Using Tabletop Rheology and Calorimetry. *Molecular Gels*; Springer: New York, 2006; pp 241−252.

(20) Peter, M.; Ganesh, N.; Selvamurugan, N.; Nair, S.; Furuike, T.; Tamura, H.; Jayakumar, R. Preparation and Characterization of Chitosan-Gelatin/Nano Hydroxyapatite Composite Scaffolds for Tissue Engineering Applications. *Carbohydr. Polym.* **2010**, *80*, 687−694.

(21) Uysal, C. A.; Tobita, M.; Hyakusoku, H.; Mizuno, H. Adipose-Derived Stem Cells Enhance Primary Tendon Repair: Biomechanical

DOI: 10.1021/acsami.5b02685
ACS Appl. Mater. Interfaces 2015, 7, 9399−9409

and Immunohistochemical Evaluation. *J. Plast. Reconstr. Aesthetic Surg.* **2012**, *65*, 1712−1719.
(22) Nakayama, G. R.; Caton, M. C.; Nova, M. P.; Parandoosh, Z. Assessment of the Alamar Blue Assay for Cellular Growth and Viability *In Vitro*. *J. Immunol. Methods* **1997**, *204*, 205−208.
(23) Liang, C. C.; Park, A. Y.; Guan, J. L. *In Vitro* Scratch Assay: A Convenient and Inexpensive Method for Analysis of Cell Migration *In Vitro*. *Nat. Protoc.* **2007**, *2*, 329−333.
(24) Soumya, S.; Sreerekha, P. R.; Menon, D.; V. Nair, S.; Chennazhi, K. P. Generation of a Biomimetic 3D Microporous Nano-Fibrous Scaffold on Titanium Surfaces for Better Osteointegration of Orthopedic Implants. *J. Mater. Chem.* **2012**, *22*, 1904−1915.
(25) Honma, T.; Senda, T.; Inoue, Y. Thermal properties and crystallization behaviour of blends of poly (ε-caprolactone) with chitin and chitosan. *Polym. Int.* **2003**, *52*, 1839−46.
(26) Jayakumar, R.; Tamura, H. Synthesis, Characterization and Thermal Properties of Chitin-*g*-Poly (ε-caprolactone) Copolymers by Using Chitin Gel. *Int. J. Biol. Macromol.* **2008**, *43*, 32−36.
(27) Kim, I. S.; Kumta, P. N. Sol-Gel Synthesis and Characterization of Nanostructured Hydroxyapatite Powder. *Mater. Sci. Eng., B* **2004**, *111*, 232−236.
(28) Senda, T.; He, Y.; Inoue, Y. Biodegradable Blends of Poly(ε-caprolactone) with α-Chitin and Chitosan: Specific Interactions, Thermal Properties and Crystallization Behavior. *Polym. Int.* **2002**, *51*, 33−39.
(29) Padmanabhan, S. K.; Balakrishnan, A.; Chu, M. C.; Lee, Y. J.; Kim, T. N.; Cho, S. J. Sol-Gel Synthesis and Characterization of Hydroxyapatite Nanorods. *Particuology* **2009**, *7*, 466−470.
(30) Rehage, H.; Hoffmann, H. Viscoelastic Surfactant Solutions: Model Systems for Rheological Research. *Mol. Phys.* **1991**, *74*, 933−973.
(31) Cross, M. M. Rheology of Non-Newtonian Fluids: A New Flow Equation for Pseudoplastic Systems. *J. Colloid Interface Sci.* **1965**, *20*, 417−437.
(32) Wei, G.; Ma, P. X. Structure and Properties of Nano-Hydroxyapatite/Polymer Composite Scaffolds for Bone Tissue Engineering. *Biomaterials* **2004**, *25*, 4749−4757.
(33) Gorbunoff, M. J.; Timasheff, S. N. The Interaction of Proteins with Hydroxyapatite: III. Mechanism. *Anal. Biochem.* **1984**, *136*, 440−445.
(34) Woo, K. M.; Seo, J.; Zhang, R.; Ma, P. X. Suppression of Apoptosis by Enhanced Protein Adsorption on Polymer/Hydroxyapatite Composite Scaffolds. *Biomaterials* **2007**, *28*, 2622−2630.
(35) Woo, K. M.; Zhang, R.; Deng, H.; Ma, P. X. Protein-Mediated Osteoblast Survival and Migration on Biodegradable Polymer/Hydroxyapatite Composite Scaffolds. *Trans. 28th Annu. Meet. Soc. Biomater.* **2002**, 605.
(36) Scherer, S. S.; Pietramaggiori, G.; Matthews, J.; Perry, S.; Assmann, A.; Carothers, A.; Demcheva, M.; MuiseHelmericks, R. C.; Seth, A.; Vournakis, J. N. Poly-n-Acetyl Glucosamine Nanofibers: A New Bioactive Material to Enhance Diabetic Wound Healing by Cell Migration and Angiogenesis. *Ann. Surg.* **2009**, *250*, 322−330.
(37) Anitha, A.; Sowmya, S.; Kumar, P. S.; Deepthi, S.; Chennazhi, K.; Ehrlich, H.; Tsurkan, M.; Jayakumar, R. Chitin and Chitosan in Selected Biomedical Applications. *Prog. Polym. Sci.* **2014**, *39*, 1644−1667.
(38) Kern, S.; Eichler, H.; Stoeve, J.; Klüter, H.; Bieback, K. Comparative Analysis of Mesenchymal Stem Cells from Bone Marrow, Umbilical Cord Blood or Adipose Tissue. *Stem Cells* **2006**, *24*, 1294−1301.
(39) Dormer, N. H.; Qiu, Y.; Lydick, A. M.; Allen, N. D.; Mohan, N.; Berkland, C. J.; Detamore, M. S. Osteogenic Differentiation of Human Bone Marrow Stromal Cells in Hydroxyapatite-Loaded Microsphere-Based Scaffolds. *Tissue Eng., Part A* **2011**, *18*, 757−767.
(40) An, S.; Ling, J.; Gao, Y.; Xiao, Y. Effects of Varied Ionic Calcium and Phosphate on the Proliferation, Osteogenic Differentiation and Mineralization of Human Periodontal Ligament Cells *In Vitro*. *J. Periodontal Res.* **2012**, *47*, 374−382.
(41) Cai, Y.; Liu, Y.; Yan, W.; Hu, Q.; Tao, J.; Zhang, M.; Tang, R. Role of Hydroxyapatite Nanoparticle Size in Bone Cell Proliferation. *J. Mater. Chem.* **2007**, *17*, 3780−3787.
(42) Beck, G. R. Inorganic Phosphate as a Signaling Molecule in Osteoblast Differentiation. *J. Cell. Biochem.* **2003**, *90*, 234−243.
(43) Fatherazi, S.; MatsaDunn, D.; Foster, B.; Rutherford, R.; Somerman, M.; Presland, R. Phosphate Regulates Osteopontin Gene Transcription. *J. Dent. Res.* **2009**, *88*, 39−44.
(44) Sila-Asna, M.; Bunyaratvej, A.; Maeda, S.; Kitaguchi, H.; Bunyaratvej, N. Osteoblast Differentiation and Bone Formation Gene Expression in Strontium-Inducing Bone Marrow Mesenchymal Stem Cell. *Kobe J. Med. Sci.* **2007**, *53*, 25−35.

DOI: 10.1021/acsami.5b02685
ACS Appl. Mater. Interfaces 2015, 7, 9399−9409